American Journal of Pathology, Vol. 151, No. 6, December 1997

Simple Epithelium Keratins Are Required for Maintenance of Hepatocyte Integrity

Anne Loranger,* Sophie Duclos,* Andrée Grenier,* Jennifer Price,† Marcia Wilson-Heiner,‡ Hélène Baribault,‡ and Normand Marceau*

From the Centre de recherche en cancérologie de l'Université Laval, L'Hôtel-Dieu de Québec, Québec, Canada; Scripps Clinic Research Institute,† La Jolla, California; and The Burnham Institute,‡ La Jolla, California*

Keratin 8 (K8)-deficient adult mice develop a severe disease of the gastrointestinal tract characterized mainly by colorectal hyperplasia and inflammation. Given that hepatocytes contain K8/K18 heteropolymers only, this animal model was used to assess the contribution of these simple epithelium keratins to hepatocyte structural and functional integrity. Homozygous mutant (HMZ), heterozygous, and wild-type (WT) mice were examined for hepatocyte structural and metabolic features and their survival to partial hepatectomy. Except for the presence of few necrotic foci, no other tissular or cellular alterations were observed in nonhepatectomized HMZ mouse livers; glycogen and lipid peroxidation levels were essentially normal, but a small reduction in bile flow was observed. In response to a single pentobarbital injection, HMZ mice had longer sleeping times than heterozygous and WT mice. After a two-thirds partial hepatectomy under pentobarbital anesthesia, all HMZ mice died within a few hours, whereas those anesthetized with ether survived for 1 to 2 days. One hour after hepatectomy after pentobarbital anesthesia, many hepatocytes contained erythrocytes and large vacuoles in the cytoplasm, which suggests damage at the plasma membrane level in response to a sudden increase in portal blood flow. In line with these findings, an uptake of trypan blue by HMZ but not WT mouse hepatocytes was observed during a 10 ml/minute perfusion via the portal vein with a dye-supplemented buffer. Subsequent cellular dispersion led to viable WT mouse hepatocytes but largely nonviable HMZ mouse hepatocytes. Better viability was obtained at lower perfusion rates. Partially hepatectomized heterozygous mice developed liver steatosis, a condition that was not associated with a change in K8 content but perhaps linked to the presence of the *neo* gene. Transgenic HMZ mouse rescue experiments with a full-length K8 gene confirmed that the phenotypic alterations observed in partially hepatectomized HMZ mice were caused by the disruption of the K8 gene. Taken together, these findings demonstrate that simple epithelium keratins are essential for the maintenance of hepatocyte structural and functional integrity. *(Am J Pathol 1997, 151:1673–1683)*

Keratins are the intermediate filament (IF) proteins of epithelial cells and consist of a multigene family of at least 20 acidic (type I) or neutral-basic (type II) peptides.[1–4] Keratin IFs are obligate heteropolymers assembled from dimers containing one polypeptide of each type.[3–5] Various keratin pairs are expressed differentially depending on the type of epithelium and its state of differentiation. For example, the K5/K14 pair is present in keratinocytes of the basal layer of stratified epithelia, whereas the terminally differentiated keratinocytes contain the K1/K10 pair.[1,2,5] In the case of simple epithelia, most cells contain the K8/K18 pair while some express, in addition, K7, K19, and/or K20.[1,3] A number of studies have clearly demonstrated that point mutations in the K1, K5, K10, or K14 gene dramatically perturb the structural integrity of keratinocytes.[4–6] Most important, these observations provide a molecular explanation for several skin diseases, such as hereditary skin-blistering disorders.[3–5] In contrast, the observations accumulated on the role of simple epithelium keratins from work performed on various nonkeratinizing tissues, including the liver, are inconclusive. For instance, simple epithelium keratins may provide mechanical strength to epithelial cells but may also be involved in signal transduction, autophagy, and programmed cell death.[7–10]

The liver is a multicellular organ in which parenchymal cells (hepatocytes) exert diverse metabolic function(s), and nonparenchymal epithelial cells (eg, biliary epithelial cells) mainly serve specialized and structural purposes.[11,12] The IFs of hepatocytes are formed by K8/K18 heteropolymers only, whereas biliary epithelial cells contain, in addition, K7 and K19,[9,13] the latter being a representative of those found in epidermal stem cells.[14] We have proposed recently that this selective pattern of ker-

Supported by a grant from the Medical Research Council of Canada to N. Marceau and a grant from the National Institutes of Health-National Institute of Arthritis and Musculoskeletal and Skin Diseases (AR41816) to H. Baribault.

Accepted for publication September 2, 1997.

Address reprint requests to Dr. Normand Marceau, Centre de recherche, L'Hôtel-Dieu de Québec, 11 Côte du Palais, Québec, Canada, G1R 2J6.

atin gene expression in hepatocytes *versus* biliary epithelial cells is functionally significant.[9]

A reliable approach to examining protein function *in vivo* is the analysis of cells or tissues that are homozygous for loss-of-function mutations as provided by targeted gene mutations introduced into the germ line of mice.[15] Recent work using this approach has shown that a K8 targeted mutation in which a neomycin (*neo*) gene was introduced into the first exon causes lethality in C57BL/6 mouse embryos with an incomplete penetrance of 94%,[16] whereas K8 gene disruption in FVB/N mice leads to colorectal hyperplasia accompanied by a pronounced inflammation of the lamina propria and submucosa after 9 weeks of age.[17] Since K18 is unable to form homopolymers, the hepatocytes of K8-deficient FVB/N mice lack K8/K18 IFs, and these mice therefore provide a unique animal model to assess the contribution of simple epithelium keratin IFs to hepatocyte structural and functional integrity.

In this study, we examined the structural integrity of hepatocytes of homozygous (HMZ) and heterozygous (HTZ) K8 mutant and wild type (WT) FVB/N mice, using both light and electron microscopy *in situ*. We also assessed the metabolic activities of the hepatocytes in terms of glycogen content, lipid peroxidation, bile production, and response to pentobarbital treatment. In parallel experiments, the three groups of mice were subjected to partial hepatectomy (PH) and to *in situ* trypan blue perfusion. In control experiments, the response to PH was assessed in neomycin-resistant (neo^R) and K8-rescued HMZ (HMZ-R) transgenic mice. The results demonstrate that the hepatocytes of K8-deficient FVB/N mice manifest increased fragility, particularly under stress conditions.

Materials and Methods

Reagents

Sodium pentobarbital was purchased from MTC Pharmaceuticals (Cambridge, Canada) and diethyl ether from Fisher Scientific (Ottawa, Canada). Lactate-Ringer solution was obtained from Abbott (Montreal, Canada). Microtubing for cannulation of the common bile duct (#6417–76) was purchased from Cole–Parmer (Montreal, Canada). Products for gel electrophoresis were obtained from Bio-Rad (Mississauga, Canada). All other chemicals were obtained from Sigma (Mississauga, Canada). The antibodies were the following: TROMA-1 and TROMA-2 rat monoclonal antibodies against mouse K8 and K18, respectively (gift from Dr. R. Kemler, Freiburg, Germany) and horseradish peroxydase-conjugated goat anti-rat Ig and Texas Red-tagged goat anti-rat IgG antibody (purchased from BIO/CAN, Mississauga, Canada).

Animals

K8-Knockout Mice

Details on the establishment of the K8-deficient FVB/N mouse line have been reported previously.[17] The genotype of each mouse was determined by polymerase chain reaction analysis of tail DNA using previously described primers.[17] The experiments were performed on 8- and 20-week-old WT, HTZ, and HMZ mice.

HMZ-R Mice

A 16-kb fragment from the mouse K8 gene, also named EndoA1α,[18] was injected into oocytes from FVB/N mice by standard procedures. A detailed characterization of these mice will be submitted for publication elsewhere. Briefly, a K8R4 mouse line carrying approximately 20 copies of the K8 rescue transgene was chosen for additional mating with the K8-knockout mice. The K8R4 mouse line expressed the K8 rescue transgene in a tissue-specific manner, although sometimes in a mosaic manner (cf. Results). The mRNA level was approximately 20-fold that of the endogenous K8 (Baribault, unpublished observations). The K8 rescue transgene was distinguished from the endogenous K8 gene by a *Xba*I site polymorphism.[17,18] K8R4 transgenic mice were apparently normal. The K8 rescue transgene was introduced into the K8 null background by additional mating of K8R4 heterozygous mice to the HMZ mice. The resulting mice carrying the K8 rescue transgene, ie, HMZ-R mice, were apparently normal, suggesting that the presence of the 16-kb K8 gene fragment and the resulting mosaic expression were sufficient to rescue HMZ mice from developing colorectal hyperplasia and from female sterility (Baribault, unpublished observations).

Neo^R Mice

These mice were a gift from Dr. T. Doetschman[19] (University of Cincinnati, OH). Briefly, the neo^R mouse line was generated by standard DNA microinjection of the pMCneopA cassette into mouse oocytes. This mouse line is used routinely to generate neo^R embryonic fibroblast feeder layers for embryonic stem cell tissue culture. The integration site of the neo^R gene is not known but is most likely different from the site of insertion into the K8 gene. The colony is maintained by regular sib-mating of homozygotes.

The animals had access to water and food *ad libitum*. All of the animal interventions were made in accordance with institutional guidelines.

Bile Flow Measurement

The common bile duct was cannulated with microtubing while the animals were under urethane anesthesia (1.1 g/kg of body weight, intraperitoneally). Body temperature was maintained by a heat lamp. Bile was collected on ice in preweighed tubes in 10 minutes aliquots for a 60-minute period and was stored at −20°C until use. Bile flow was measured gravimetrically, assuming a density of 1 g/ml.[20,21]

Partial Hepatectomy

The mice were subjected to PH[22] under anesthesia via a sodium pentobarbital (54 mg/kg of body weight) intraperitoneal injection or an exposure to ether. Careful asepsis was maintained throughout all operations. Through a median-line incision posteriorly from the xiphoid process of the sternum, the large median lobe with the left lateral lobe were ligated and then excised. The portion removed corresponded to two-thirds of the total liver, leaving the right lateral lobe and the small caudate lobe. In some experiments, one-third PH was performed by removing the median lobe only. Before and after the surgery, the mice received 0.3 ml of lactate-Ringer solution subcutaneously. The ambient temperature was maintained at 25°C with a thermostated pad placed under the animals during the surgical procedure and under the cages during the period after the hepatectomy. The livers from all genotypes were examined before PH and during the next 3 days after the PH. Mice that were alive at day 3 after the PH were killed at day 12 to monitor the overall structural and metabolic status of their livers.

Liver Perfusion and Hepatocyte Isolation

The liver was perfused according to a modified version of the two-step method with collagenase originally developed for rats.[23,24] The mouse was anesthetized with ether and the abdominal cavity was opened to cannulate the vena portalis and to section the vena cava.[24] The liver was first perfused at 37°C with a Ca^{++}-free *N*-2-hydroxyethyl piperazine-*N'*-2-ethanesulfonic acid buffer[23] and thereafter with the same buffer containing 0.025% collagenase and 5 mmol/L Ca^{++}. In both cases, the buffer was supplemented with 0.4% trypan blue to assess the capacity of the hepatocytes to exclude the dye under perfusion at a flow rate of 5 or 10 ml/minute. The liver tissue was processed as described below except that the morphological features were examined on sections counterstained with 1% Eosin Y only. Under light microscopy, a trypan blue-positive hepatocyte had a typically blue nucleus and a pink cytoplasm. In parallel experiments, the two-step perfusion was conducted in the absence of trypan blue and the hepatocytes were dispersed, as described before.[23] The yield of isolated hepatocytes was determined with an hemacytometer, and their viability evaluated with the standard trypan blue exclusion assay.[24]

Morphological Analyses

Histology

Liver tissue slices were fixed in 10% (v/v) neutral formalin, embedded in paraffin, and stained with hematoxylin and eosin (H&E).[20,21]

Fluorescence Microscopy

Small pieces of liver were embedded in OCT, frozen in liquid nitrogen, and then processed for cryostat sectioning.[25] Frozen sections were laid out on slides, air-dried, and fixed in 100% acetone at −20°C for 10 minutes. Sections were then incubated overnight at 4°C with rat monoclonal antibodies directed against K8 (TROMA-1) and K18 (TROMA-2)[17,18] and followed by the second reaction involving a 60-minute incubation at room temperature with a Texas Red-labeled anti-rat immunoglobulin antibody. Lipids were detected by Nile Red staining. A stock solution of Nile Red (500 mg/ml) in acetone was prepared and stored chilled in the dark. A fresh staining solution of Nile Red was made by the addition of 10 ml of the stock solution to 1 ml of 75% glycerol, followed by vortexing.[21] A drop of stain was added to the tissue sections and the preparations were covered with glass coverslips. The sections were examined after 5 minutes. Fluorescence microscopy was performed with a Bio-Rad MRC-600 confocal laser scanning microscope equipped with a krypton-argon laser beam using the excitation lines 488 and 514 nm. Confocal images were obtained using a high numerical aperture (1.3 NA, 40X) oil immersion objective and appropriate zoom factors. After contrast enhancement, images were printed with a UR5100 videoprinter.[25] In the case of HMZ-R mouse liver, the percentage of K8/K18-positive hepatocytes was estimated by counting the number of pixels in positive *versus* whole areas in three fields (200 cells per field) taken at random on five tissue slides from different lobes.

High Resolution Light Microscopy (HRLM) and Electron Microscopy (EM)

Small pieces of liver were fixed overnight at 4°C in universal fixative (1% glutaraldehyde, 4% paraformaldehyde in sodium phosphate buffer, pH 7.2).[26] The tissue blocks were then postfixed in 1% OsO_4 in Sorensen's buffer, dehydrated in a graded ethanol series, and embedded in Araldite. Representative sections 0.5 to 1.0 mm thick were cut for HRLM, stained with toluidine blue, and examined with a Nikon Optiphot-2 light microscope. Ultrathin sections were also cut, stained with uranyl acetate and lead citrate, and examined with a Jeol 1200CX electron microscope.

Biochemical Measurements

The glycogen content in the liver was determined by colorimetric measurement of an anthrone color reaction at 660 nm.[27] Lipid peroxydation was evaluated by the thiobarbituric acid-reactive substances assay.[28] The level of thiobarbituric acid-reactive substances was calculated by the difference between optical density 535 and 520 nm.

Western Blotting

Total proteins were obtained by homogenizing the liver tissue in buffer consisting of 96 mmol/L NaCl, 8 mmol/L KH_2PO_4, 5.6 mmol/L $Na_2PO_4 \cdot 2\ H_2O$, 1.5 mmol/L KCl, 10 mmol/L ethylenediaminetetraacetic acid, 0.1 mmol/L DL-dithiothreitol, pH 6.8, containing protease inhibitors (1

mmol/L phenylmethylsulfonyl fluoride, 5 mmol/L ethylenediaminetetraacetic acid, 1 mmol/L pepstatin, 1 mmol/L leupeptin, 0.3 mmol/L aprotinin) and phosphatase inhibitors (2 mmol/L NaF, 2 mmol/L Na_3NO_4, 20 mmol/L $Na_2MoO_4 \cdot 2\ H_2O$).[19,25] Total proteins (30 μg) solubilized in sodium dodecyl sulfate were fractionated by polyacrylamide gel electrophoresis according to Laemmli.[29,30] The proteins were then electrophoretically transferred onto nitrocellulose sheets[31] and the blots were incubated with the rat anti-mouse K8 (TROMA-1) or K18 (TROMA-2) antibodies. The second antibody was a horseradish peroxydase-conjugated goat anti-rat Ig, and the detection involved the ECL Western blotting detection system (Amersham, Montreal, Canada), as described before.[25,32]

Results

Unless otherwise stated, all of the data reported here are derived from experiments performed on 20-week-old mice. This age was chosen on the basis of previous findings showing that the overall phenotype appears predominantly after 9 weeks of age in the FVB/N mouse background.[17]

Liver Structural and Functional Features

The overall assessment of the histological features after H&E staining revealed no alteration in the WT and HTZ mouse livers (Figure 1, a and d) but did reveal some lipofuscin inclusions and necrotic foci in HMZ mouse livers (Figure 1g). As previously reported and as expected, K18 containing IFs were present in WT and HTZ mouse livers (Figure 1, b and e), whereas they were found only in the bile duct structures in HMZ mouse livers (Figure 1h).

To determine the relationship between K8 deficiency and hepatocyte structural integrity, the livers of WT, HTZ, and HMZ mice were examined at the EM level. Essentially all of the typical ultrastructural features observed in WT mouse liver, such as cytoplasmic organelle shape and distribution and presence of cell-cell junctions (Figure 1c), remained unperturbed in HTZ and HMZ mouse livers (Figure 1, f and i). Therefore, the lack of keratin IFs is not deleterious to the overall ultrastructure of hepatocytes under nonstress conditions.

To assess the overall metabolic status of the liver, we first determined the level of glycogen in the livers of WT, HTZ, and HMZ mice (Table 1). Overall, the results indicate that there is no major difference in the glycogen level among the various groups.

Liver damage is often linked to lipid peroxidation,[33] and it was therefore of interest to assess this parameter in WT, HTZ, and HMZ mouse livers. As shown in Table 1, there was no difference among the three groups, which shows that the appearance of lipofuscin inclusions and necrotic foci in HMZ mouse liver cannot be explained by alterations in liver oxidative status.

We next examined the capacity of the hepatocytes to produce bile, a major liver function that requires the contribution of cytoplasmic membranous compartments, cytoskeletal elements, and specialized cell surface membrane domains.[34,35] As shown in Table 1, a 20% reduction in bile flow was observed with HMZ mice when compared with the WT group, which suggests a keratin involvement in this hepatocyte metabolic activity.

The liver is the major detoxifying organ, and we assessed this metabolic feature by administrating a single anesthetic dose of pentobarbital to WT, HTZ, and HMZ mice and by determining the time required for them to awaken (Table 1). Whereas both WT and HTZ mice awoke after approximately 100 minutes, HMZ mice did not awake before 170 minutes. This suggests that the loss of keratin IFs might affect the elimination of xenobiotic agents.

Mouse Survival after Partial Hepatectomy

PH is a classical means for inducing liver regeneration.[36] This dramatic insult triggers a rapid proliferation of the hepatocytes, whereas the remnant tissue must be able to maintain its capacity to perform metabolic activities and to resist a sudden increase in blood flow; failure results in death of the animal. In a first set of experiments, mice were anesthetized with pentobarbital and subjected to two-thirds PH. As expected (Table 2), most of the WT and HTZ mice recovered from the operation, which the survival between the two groups was comparable. However, none of the HMZ mice survived (Table 2), death occurred within the first hours after PH. Of the eight mice studied, four died at 1 hour, three died at 3 hours, and one died at 6 hours.

Because the sleeping time of HMZ mice anesthetized with pentobarbital was much longer than that of WT mice (Table 1), the differential survival after PH among mice of the three genotypes could be due to a differential capacity of the mixed-function oxydase system and conjugation reaction to metabolize and conjugate the drug.[37] To test this possibility, the next set of two-thirds PHs was performed on mice anesthetized with ether, an agent that is not eliminated through the liver.[38] Although none of the seven HMZ mice were able to survive the 3-day period after PH (Table 2), four stayed alive for 1 to 2 days, suggesting that part of the response to PH was dependent on the ability of the hepatocytes to metabolize the anesthetic agent. HTZ and WT mice were not affected by the type of anesthetic, ie, both groups survived very well (Table 2).

Observations made on the emergence of the colorectal phenotype indicated that alteration of gut structure occurred progressively and increased with age.[17] Thus, it was of interest to determine the PH-induced response in younger mice. At 8 weeks of age, four of eight HMZ mice anesthetized with pentobarbital survived the operation, and the death of the other four mice was delayed to 19 to 26 hours (data not shown). Together with the data on the 20-week-old mice, the present findings indicate that the capacity of HMZ mice to survive after PH decreased with age.

To better define the range for the survival capacity after PH, HMZ mice were subjected to one-third PH. Eight

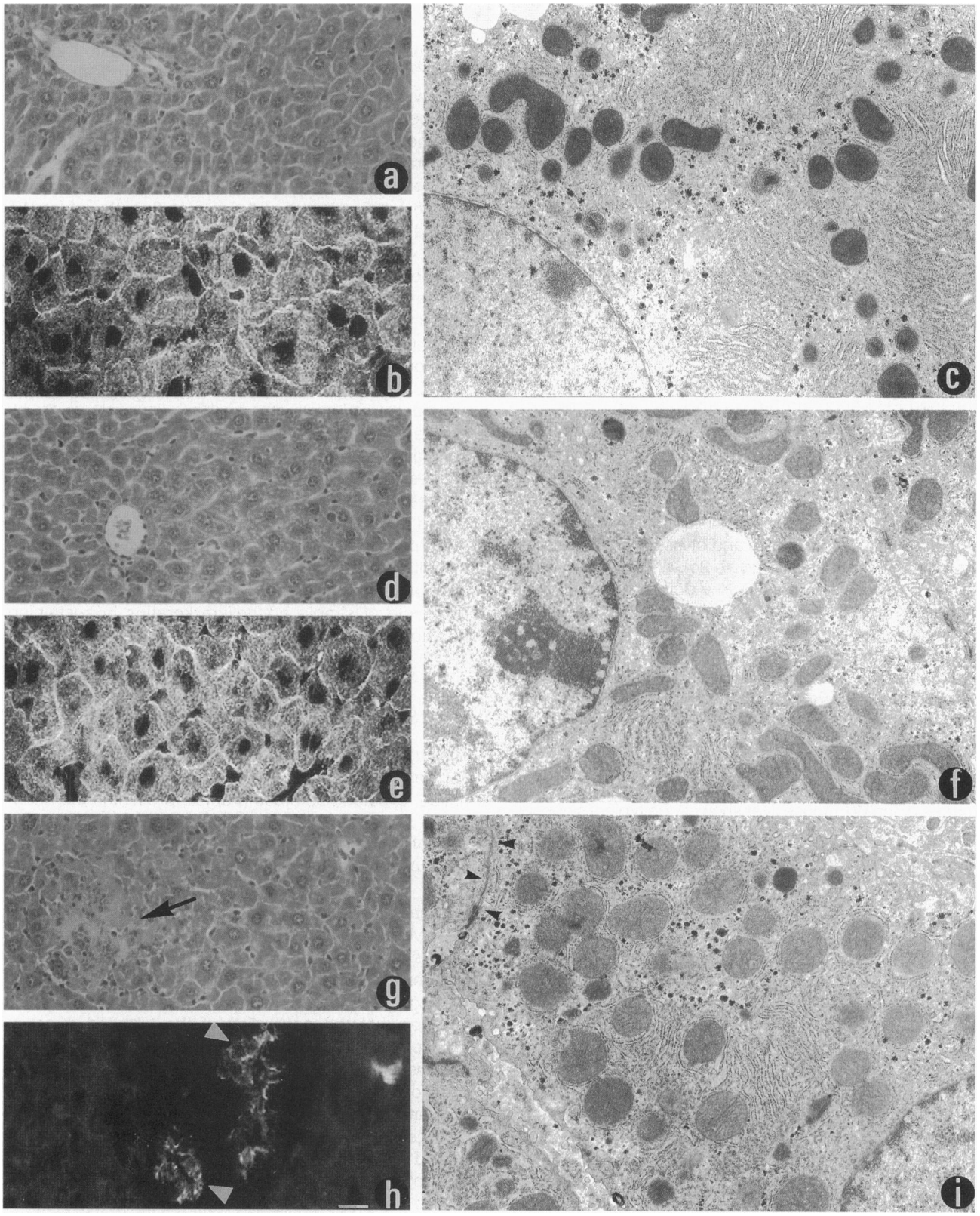

Figure 1. H&E staining (**a, d,** and **g**), immunofluorescence microscopy of K18 (**b, e** and **h**), and electron microscopy (**c, f,** and **i**) of liver tissue from WT (**a, b,** and **c**), HTZ (**d, e,** and **f**), and HMZ (**g, h,** and **i**) mice. The **arrow** points to hepatocyte necrosis (**g**). Note also the presence of K18 in biliary epithelial cells (**white arrowheads**) of HMZ mice (**h**). Hepatocytes from the three genotypes show no alteration of the various organelles. All genotypes exhibit junctional complexes at the basolateral membrane (eg, **small arrowheads** in **i**). Magnification, ×400 (**a, d,** and **g**) and ×6500 (**c, f,** and **i**). Scale bar, 10 μm (**b, e,** and **h**).

Table 1. Metabolic Status of the Mouse Livers

Parameters	WT	HTZ	HMZ
Glycogen (g/10 g of liver)	2.3 ± 0.5	1.6 ± 0.6*	2.0 ± 0.7
Lipid peroxidation (TBARS)	0.04 ± 0.01	0.04 ± 0.01	0.03 ± 0.003
Bile flow (μl/minute/g of liver)	1.67 ± 0.29	n.d.	1.22 ± 0.19†
Sleeping time (minute)§	106.3 ± 6.5	100.5 ± 5.4	171.5 ± 15.7‡

The number of mice is 6 to 9.
Abbreviations: §, 90 mg/kg·pentobarbital anesthesia; n.d., not done; TBARS, thiobarbituric acid-reactive substances.
*, $P < 0.06$; †, $P < 0.0001$; ‡, $P < 0.016$.

of nine mice were alive at day 3 after the HP. A second one-third PH performed 3 days after the first PH did not affect survival.

Liver Morphology after Partial Hepatectomy

We inspected the gross morphology of WT mouse livers at 3 days (Figure 2, a and b) and of HMZ mouse livers at 1 hour after two-thirds PH (Figure 2c). WT livers were light red, whereas the HMZ livers were dark red. Histological examination confirmed that the features of the WT mouse liver at 1 hour after the two-thirds PH (Figure 1d) were essentially identical to those at later times or to those of nonhepatectomized WT mouse livers (Figure 1a). However, massive hemorrhage was present in HMZ mouse livers at 1 hour after the PH (Figure 2f) and at later times (data not shown).

We performed HRLM and EM analyses on WT and HMZ liver sections at 1 hour after the PH. The HRLM images of the WT mouse liver showed the typical sinusoid and hepatocyte compartments with erythrocytes aligned in the sinusoids, whereas those of the HMZ mouse liver revealed the presence of small erythrocyte clumps among many disrupted hepatocytes (data not shown). The EM pictures additionally documented these observations. Although the ultrastructure of WT mouse hepatocytes remained largely unaffected in response to the PH (compare Figure 3a with Figure 1c), erythrocytes and large vacuoles were observed in the cytoplasm of HMZ mouse hepatocytes (Figure 3b). Overall, the bile canaliculi were undisturbed with the junctional complexes being present (Figure 3b, insert).

In mice able to survive the 3-day period after the PH, no differences in growth recovery and tissue organization of the regenerating livers were observed.

Table 2. Survival after Two-Thirds Partial Hepatectomy

Anesthesia	WT	HTZ	HMZ	neo^R	HMZ-R
Pentobarbital	4/5	5/9	0/8	n.d.	n.d.
Ether	6/7	13/18	0/7	4/5	3/5

*, Mice that survived at 3 days after PH/total; n.d. = not determined.

Hepatocyte Viability after in Situ *Perfusion*

The well established hepatocyte isolation procedure,[23,24] which involves a washing perfusion of the liver with a Ca^{++}-free buffer and a second perfusion with collagenase and Ca^{++}, was used as an assay to test the hepatocyte resistance to mechanical stress. A washing perfusion at a flow rate of 10 ml/minute for 5 minutes followed by collagenase perfusion at 5 ml/minute for 6 minutes did not significantly affect WT mouse hepatocytes (Figure 4a) but massively damaged HMZ mouse hepatocytes (Figure 4b). Many hepatocytes exhibited necrotic features as shown by trypan blue staining. The overall damage observed in HMZ mouse hepatocytes was similar to that seen after PH (Figure 2f). It should be noted that a comparable level of damage was already observed after perfusion with Ca^{++}-free buffer alone. Less damage was observed by reducing the washing flow rate to 5 ml/minute (data not shown). Under the latter perfusion condition, the viability of the isolated WT mouse hepatocytes was 92%, whereas that of HMZ mouse hepatocytes was 42% (Table 3). In line with the data obtained after PH, a two-step collagenase perfusion performed on 8-week-old mice yielded hepatocytes exhibiting a viability of 66% (data not shown). This loss of hepatocyte structural integrity in HMZ mice argues for a role of simple epithelium keratins in sustaining hepatocyte mechanical strength.

Liver Steatosis after Partial Hepatectomy

The livers of HTZ mouse livers at 3 days after two-thirds PH were of beige color (Figure 2b). Histological examination revealed numerous droplets present in the hepatocyte cytoplasm (Figure 2e); these droplets were stained with Nile Red and hence contained lipids (data not shown). HMZ mice that survived for 1 to 2 days after PH under either anesthesia developed liver steatosis, whereas none of the surviving WT mice did (Table 4). The K8 levels were essentially the same in HTZ and WT mouse livers before or after PH (Figure 2g). Thus, the accumulation of lipids was not associated with a change in K8 content.

Given that the generation of the targeted mutation involved the integration of the *neo* gene at the K8 locus, the possible contribution of this new gene to the appearance of liver steatosis was tested. To this end, complementary experiments were performed with a different transgenic neo^R mouse line carrying a randomly integrated *neo* gene. The K8/K18 content and IF distribution in neo^R hepatocytes were equivalent to those of WT mouse hepatocytes (Figure 5 and data not shown). Moreover, only one of five neo^R mice died after two-thirds PH (Table 2), and the animal had developed liver steatosis (Table 4). By extension, this observation raises the possibility that the integrated *neo* gene may contribute to the accumulation of lipids in HTZ and HMZ mouse hepatocytes.

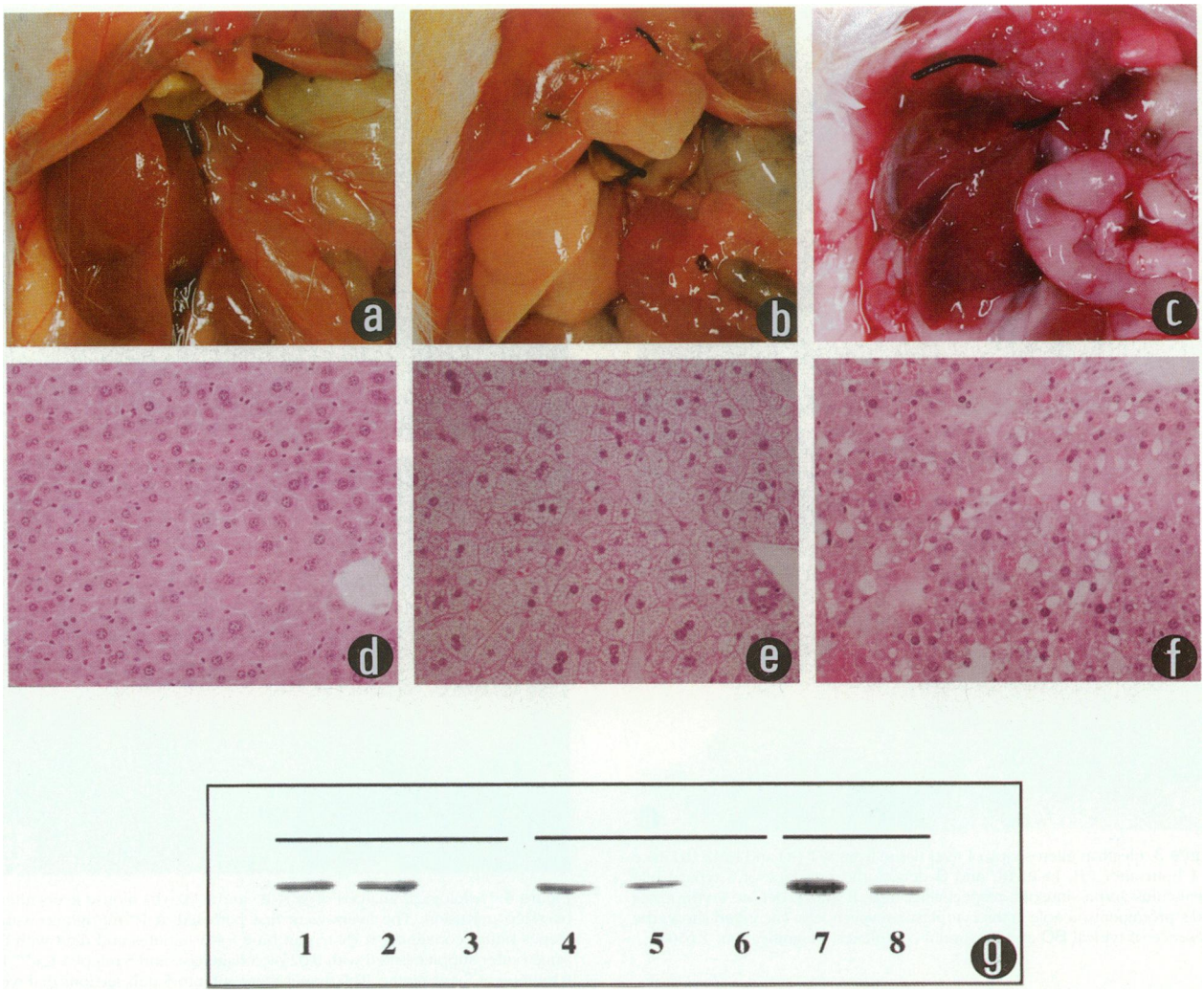

Figure 2. Analysis of liver tissue from WT and HTZ mice at 3 days after PH and HMZ mice at 1 hour after PH. Note the differences in gross morphology among WT (**a**), HTZ (**b**), and HMZ (**c**) mouse livers. In the case of WT and HTZ mice, the remaining lobes have regained 75% of the original organ volume. Moreover, the HTZ mouse livers exhibit steatosis. In the case of HMZ mice, the remaining lobes have turned darker and look swollen (**c**) when compared with that of the lobes from WT mice at the same time after PH (not shown). The H&E staining demonstrates major differences at both tissue and cell levels. The histological features of regenerating WT mouse livers (**d**) are comparable with those of nonhepatectomized WT mouse livers (Figure 1a). Regenerating HTZ mouse livers exhibit many lipid droplets accumulated in hepatocyte cytoplasm (**e**), which stain with Nile Red (not shown). At 1 hour after PH, prominent HMZ mouse hepatocyte damage, characterized by vacuolization and hemorrhagic necrosis, is observed. **g** shows K8 Western blots after sodium dodecyl sulfate-polyacrylamide gel electrophoresis fractionation of total proteins from WT (**1, 4,** and **7**), HTZ (**2, 5,** and **8**), and HMZ (**3** and **6**) mouse livers before and after PH. **Lanes 1** to **3** show the results obtained at time 0, whereas **lanes 4 to 6** and provide data observed at 6 hours and lanes **7** and **8** at 24 hours. Magnification, ×400 (**d** to **f**).

Restoration of the Phenotype in K8-Deficient Mice

Rescue experiments were performed using a HMZ-R mouse line, ie, transgenic HMZ mice carrying a full-length randomly integrated K8 gene (see Material and Methods for details). Immunofluorescence analysis revealed that 83 ± 1.3% of the HMZ-R mouse hepatocytes were K8/K18 positive. Despite this incomplete rescue, the K8/K18 content and IF distribution in HMZ-R mouse hepatocytes were essentially restored to those observed in WT mouse hepatocytes (Figure 5 and data not shown). Moreover, in contrast to the lethality observed with HMZ mice after two-thirds PH, three of five HMZ-R mice survived at 3 days and the other two died at 1 day after the PH (Table 2), thus demonstrating that the reinsertion of K8 into HMZ mice can restore the survival after PH.

Discussion

The present results demonstrate that simple epithelium keratins are involved in the maintenance of structural and functional integrity of K8-deficient FVB/N mouse hepatocytes, a conclusion that is based on the hepatocyte fragility observed in response to a two-thirds PH and to a portal perfusion. Moreover, the differential survival observed after PH performed under pentobarbital *versus* ether anesthesia in HMZ mice suggests that death could also be due in part to the inability of the remnant hepa-

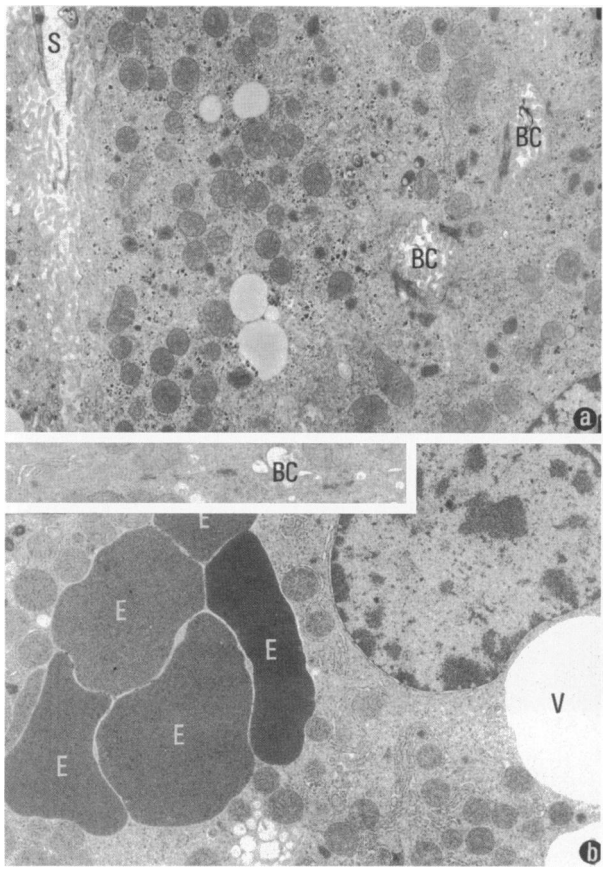

Figure 3. Electron microscopy of liver tissue from WT (**a**) and HMZ (**b**) mice at 1 hour after PH. In **a**, BC and **S** denote the presence of a typical bile canaliculus and a sinusoid, respectively. In **b**, **E** and **V** denote erythrocytes and a prominent vacuole in the cytoplasm, respectively. The **insert** shows the presence of typical **BC** and junctional complexes. Magnification, ×6500.

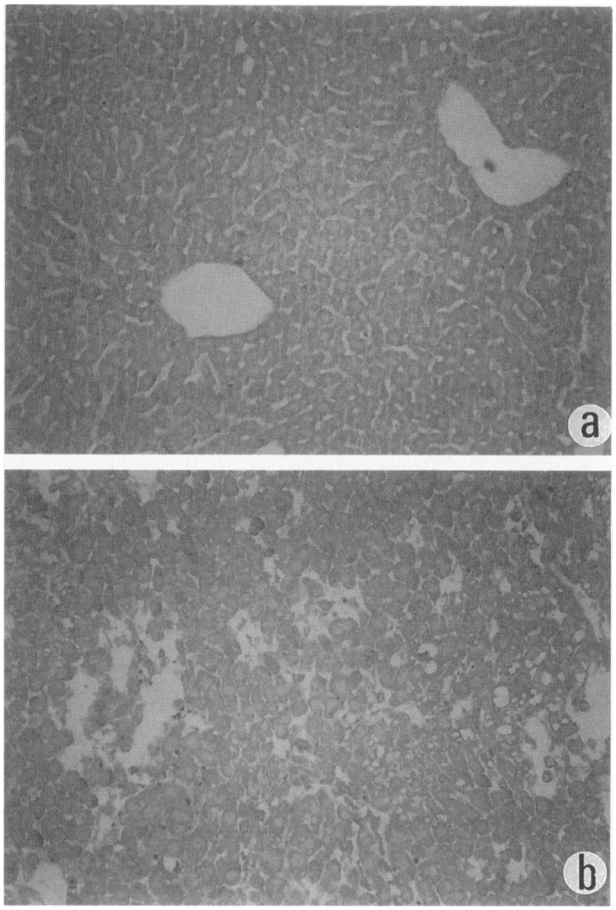

Figure 4. Histological analysis of WT (**a**) and HMZ (**b**) mouse livers after a two-step perfusion. The livers were first perfused at 10 ml/minute with a Hepes buffer containing 0.4% trypan blue for 5 minutes and then with the same buffer supplemented with 0.025% collagenase and 5 mmol/L Ca^{++} for 6 minutes at 5 ml/minute. The tissues were cut into 5-mm sections that were counterstained with 1% eosin Y. Note that the overall cellular damage observed is somewhat comparable with that seen after PH (Figure 2f). Many hepatocytes exhibit necrotic features, which include the presence of trypan blue-stained nuclei (eg, dark nuclei in empty spaces).

tocytes to cope with a toxic stress. The reinsertion of K8 into HMZ mouse hepatocytes can rescue the normal phenotype. K8-deficient mice provide a new animal model for studying the underlying role of keratin IFs in the genesis of chronic liver diseases.

The present data on the ultrastructure of hepatocytes in K8-deficient mice demonstrate a vital requirement for simple epithelium keratins that is similar to that of epidermal keratins. For example, nonhepatectomized K8-deficient mouse hepatocytes show no sign of gross structural alterations at the levels of the plasma membrane or the various organelles. Similar observations have also been made on transgenic mice that express K14 ectopically in the liver.[7] In the same way, keratinocytes that contain epidermal keratins carrying point mutations remain ultrastructurally unaffected.[6] However, with both hepatocytes and keratinocytes, the requirement of keratins for the maintenance of structural integrity becomes most obvious under stress conditions.

The massive damage observed in HMZ mouse hepatocytes in response to a two-thirds PH or a portal perfusion suggests that a lack of keratin IFs makes the plasma membrane more fragile. In both cases, the membrane seems unable to support an increase in fluid pressure generated in the sinusoidal space. In the same way, we have shown recently a single injection of phalloidin to normal rats or mice is sufficient to generate transient hepatocyte damage that resembles that observed in HMZ mouse hepatocytes after two-thirds HP, ie, plasma membrane vacuolization and hemorrhagic necrosis.[39] On these grounds, our working hypothesis is that actin microfilaments and K8/K18 IFs might have a cooperative function in providing strength to the membrane and that perturbing one or the other leads to increased membrane malleability.

Bile formation and secretion depend on a complex interplay among intrahepatocytic transport, tight junction permeability, plasma membrane carriers, and bile cana-

Table 3. Hepatocyte Yield and Viability Following a Two-Step Liver Perfusion with Collagenase at 5 ml/minute

Isolated hepatocytes	WT	HMZ
Yield (× 10^7 liver)*	8.2 ± 1.8	2.5 ± 0.4†
Viability (%)	92 ± 1.6	42 ± 3.7†

*, Number of mice is 5; †, $P < 0.0001$.

Table 4. Liver Steatosis after Two-Thirds Partial Hepatectomy

Anesthesia	WT	HTZ	HMZ	neo^R	HMZ-R
Pentobarbital	0/5*	6/9	n.s.	n.d.	n.d.
Ether	0/7	3/18	4/7	1/5	2/5

*, Mice with liver steatosis/total; n.s., no survival; n.d., not determined.

licular contractility.[40] In turn, this dynamic interplay is linked to the participation of cytoskeletal elements. For example, the data accumulated on the effect of microtubule-disrupting agents, such as colchicine, indicate that microtubules are involved in transcellular transport,[40] whereas those on the effect of phalloidin, a toxin that binds to actin microfilaments and impairs depolymerization, suggest that actin regulates bile canalicular contraction.[34,35] The evidence for the involvement of keratins in the regulation of bile flow is still fragmentary, and the main reason is that no agents with similar perturbing activity are available for keratin IFs. Nevertheless, the present findings with K8-deficient mice, showing a significant reduction in bile flow, indicate that keratins IFs contribute to this cytoskeletal interplay.

The present results indicate that the pentobarbital metabolism is perturbed in HMZ mouse hepatocytes, and at first sight, the link between keratin IF status and xenobiotic biotransformation is not obvious. However, in cultured hepatocytes exposed to phenobarbital and other xenobiotics, it seems clear that the induction of cytochromes P450 is highly dependent on the integrity of microtubules and actin microfilaments.[41] In light of the interplay taking place among keratin IFs and these other cytoskeletal elements, a lack of keratins in HMZ mouse hepatocytes could well result in perturbed xenobiotic metabolism.

The phenotype described here for K8-deficient mouse liver is different from that observed recently in arg89→cys K18 transgenic mice,[8] and this observation may provide clues to human pathologies. Whereas in both K8-deficient mice and arg89→cys K18 transgenic mice the hepatocytes are more fragile, no disruption in the colon has been observed in the latter case. This can be explained by the fact that K19 and K20 are present in enterocytes, and consequently normal K8/K19 and K8/K20 simple epithelium keratin IFs extending throughout the cytoplasm are still intact.[8,17] This would then argue for some functional overlap among the simple epithelium type I keratins present in enterocytes. In the case of hepatocytes, a K8/K18 IF deficiency induces alterations at the organ level that differ greatly from those observed in response to a massive keratin IF perturbation. For example, in contrast to the low level of inflammation observed in K8-deficient mouse liver, a chronic inflamma-

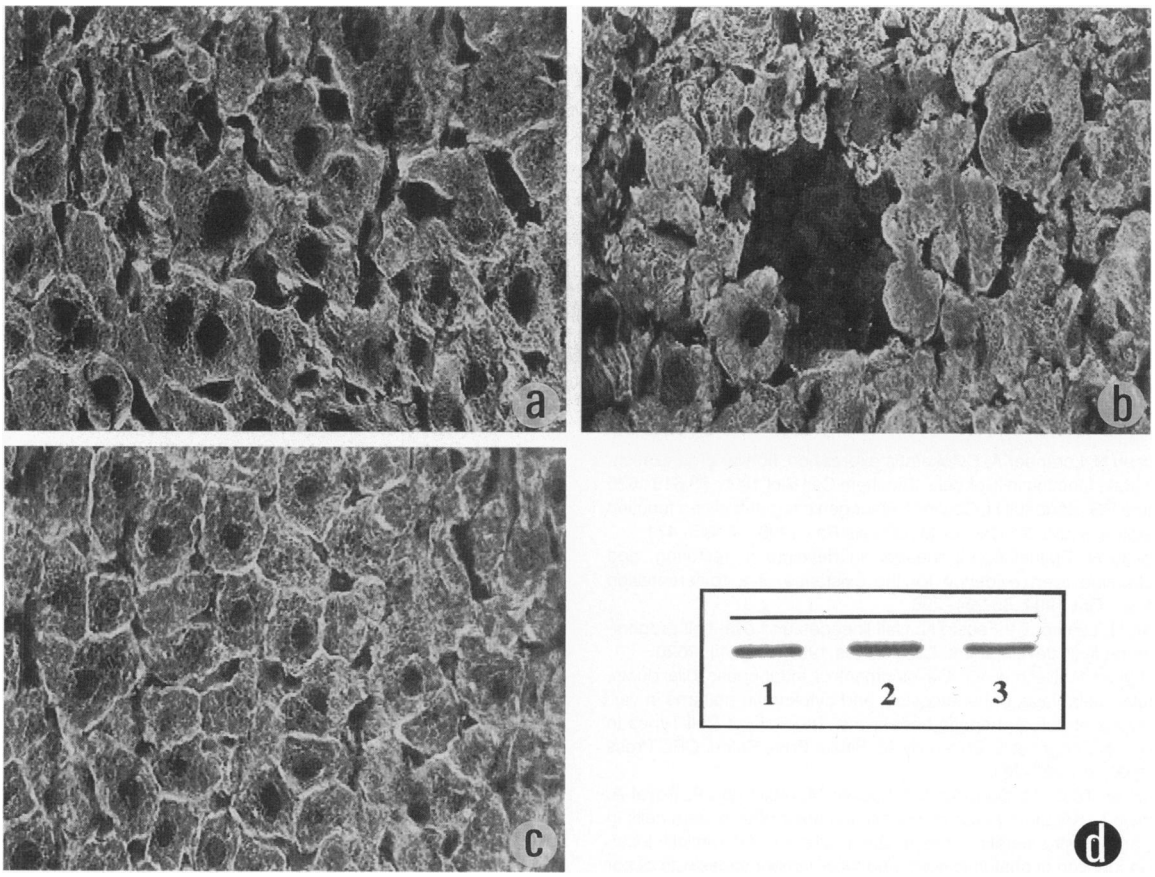

Figure 5. Immunofluorescence microscopy (**a** to **c**) and Western blotting (**d**) of K8 in neo^R (**a** and **d**, lane 1), HMZ-R (**b** and **d**, lane 2), and WT (**c** and **d**, lane 3) mouse livers. Note that the keratin IF distributions in neo^R and HMZ-R are comparable with that in WT mouse hepatocytes. In the same way, the content of K8 in neo^R and HMZ-R (considering a 83% rescue) mouse hepatocytes is equivalent to that in WT mouse hepatocytes. Scale bar, 10 μm.

tion was reported in arg89→cys K18 transgenic mouse liver.[8] In this way, the two types of mice provide complementary animal models for the genesis of various liver pathologies. In this regard, a K18 mutation (his127→leu) was recently identified in a patient with cryptogenic cirrhosis,[42] implying that K8 mutations might be also involved in chronic liver diseases of unknown etiology.[43,44] If this is the case, perturbations in simple epithelium keratin differential expression and fibrillar organization could be instrumental in the pathogenesis of some common human liver diseases.

Acknowledgments

We are grateful to Dr. R. Kemler for the generous gift of TROMA-1 and TROMA-2 hybridomas and Dr. T. Doetschman for the neo^R transgenic mouse line. We also thank Drs. J. Huot, R. G. Oshima, and S. Schaefer for helpful discussions, Dr. Alan Anderson for critical reading of the manuscript, and R. Jenkins and W. Charbono for animal husbandry.

References

1. Moll R, Franke WW, Schiller DL, Geiger B, Krepler R: The catalog of human cytokeratins: patterns of expression in normal epithelia, tumors and cultured cells. Cell 1982, 31:11–24
2. Fuchs E, Weber K: Intermediate filaments: structure, dynamics, function and disease. Annu Rev Biochem 1994, 63:345–382
3. Oshima RG: Intermediate filament molecular biology. Curr Opin Cell Biol 1992, 4:110–116
4. McLean WHI, Lane EB: Intermediate filaments in disease. Curr Opin Cell Biol 1995, 7:118–125
5. Steinert PM: Structure, function, and dynamics of keratin intermediate filaments. J Invest Dermatol 1993, 100:729–734
6. Coulombe PA, Fuchs E: Molecular mechanisms of keratin gene disorders and other bullous diseases of the skin. Molecular Mechanisms in Epithelial Cell Junctions: From Development to Disease. Edited by S Citi. Austin, RG Landes Co, 1994, pp 259–285
7. Alberts KM, Davis FE, Perrone TN, Lee EY, Liu Y, Vore M: Expression of an epidermal keratin protein in liver of transgenic mice causes structural and functional abnormalities. J Cell Biol 1995, 128:157–169
8. Ku NO, Michie S, Oshima RG, Omary MB: Chronic hepatitis, hepatocyte fragility, and increased soluble phosphoglycokeratins in transgenic mice expressing a keratin 18 conserved arginine mutant. J Cell Biol 1995, 131:1303–1314
9. Marceau N, Loranger A: Cytokeratin expression, fibrillar organization, and subtle function in liver cells. Biochem Cell Biol 1995, 73:619–625
10. Oshima RG, Baribault H, Caulin C: Oncogenic regulation and function of keratins 8 and 18. Cancer Metastasis Rev 1996, 15:445–471
11. Marceau N: Epithelial cell lineages in developing, restoring, and transforming liver: evidence for the existence of a "differentiation window". Gut 1994, 35:294–296
12. Shiojiri N, Lemire JM, Fausto N: Cell lineages and oval cell progenitors in rat liver development. Cancer Res 1991, 51:2611–2620
13. Van Eyken P, Desmet VJ: Development of intrahepatic bile ducts, ductular metaplasia of hepatocytes, and cytokeratin patterns in various types of human hepatic neoplasms. The Role of Cell Types in Hepatocarcinogenesis. Edited by AE Sirica. Boca Raton, CRC Press Inc, 1992, pp 227–264
14. Michel M, Török N, Godbout MJ, Lussier M, Gaudreau P, Royal A, Germain L: Keratin 19 as a biochemical marker of skin stem cells in vivo, and in vitro: keratin 19 expressing cells are differentially localized in function of anatomic sites, and their number varies with donor age, and culture stage. J Cell Sci 1996, 109:1017–1028
15. Rossant J, Joyner AL: Towards a molecular-genetic analysis of mammalian development. Trends Genet 1989, 5:277–283
16. Baribault H, Price J, Miyai K, Oshima RG: Mid-gestational lethality in mice lacking keratin 8. Genes Dev 1992, 7:1991–2002
17. Baribault H, Penner J, Iozzo RV, Wilson-Heiner M: Colorectal hyperplasia and inflammation in keratin 8-deficient FVB/N mice. Genes Dev 1994, 8:2964–2973
18. Vasseur M, Duprey P, Brulet P, Jacob F: One gene and one pseudogene for the cytokeratin endo A. Proc Natl Acad Sci USA 1985, 82:1155–1159
19. Shull MM, Ormsby I, Kier AB, Pawlowski S, Diebold RJ, Yin M, Allen R, Sidman C, Proetzel G, Calvin D: Targeted disruption of the mouse transforming growth factor-β 1 gene results in multifocal inflammatory disease. Nature 1992, 359:693–9
20. Loranger A, Barriault C, Youseff I, Tuchweber B: Structural and functional alterations of hepatocytes during transient phalloidin-induced cholestasis in the rat. Toxicol Appl Pharmacol 1996, 137:100–111
21. Loranger A, Tuchweber B, Youseff I, Marceau N: Biliary secretion and actin-cytokeratin filament distribution in rat hepatocytes during phalloidin-induced cholestasis. Biochem Cell Biol 1995, 73:641–649
22. Higgins GM, Anderson RM: Experimental pathology of the liver: I. restoration of the liver of the white rat following partial surgical removal. Arch Path 1931, 12:186–202
23. Seglen PO: Preparation of isolated rat liver cells. Methods in Cell Biology. Edited by D Prescott. New York, Academic Press, 1976, pp 29–83
24. Deschênes J, Valet JP, Marceau N: Hepatocytes from newborn and weanling rats in monolayer culture: isolation by perfusion fibronectin-mediated adhesion, spreading, and functional activities. In Vitro 1980, 16:722–730
25. Blouin R, Blouin MJ, Royal I, Grenier A, Roop DR, Loranger A, Marceau N: Cytokeratin 14 expression in rat liver cells in culture, and localization in vivo. Differentiation 1992, 52:45–54
26. Mc Dowell EM, Trump BF: Histologic fixatives suitable for diagnosis light and electron microscopy. Arch Pathol Lab Med 1976, 100:405–414
27. Brixova E, Dzurikova V: Determination of glycogen, lipids and proteins in hepatic needle biopsy. Clin Chim Acta 1972, 36:543–548
28. Uchiyama M, Mihara M: Determination of malonaldehyde precursor in tissues by thiobarbituric acid test. Anal Biochem 1978, 86:271–278
29. Laemmli UK: Cleavage of structural proteins during the assembly of the head of bacteriophage T4. Nature 1970, 227:680–685
30. Royal I, Gourdeau H, Blouin R, Marceau N: Down-regulation of cytokeratin 14 mRNA in polyoma virus middle T-transformed rat liver epithelial cells. Cell Growth Differ 1992, 3:589–596
31. Towbin H, Stochelen T, Gorden H: Electrophoretic transfer of proteins from polyacrylamide gels to nitrocellulose sheets: procedure and some applications. Proc Natl Acad Sci USA 1979, 76:1350–1354
32. Royal I, Raptis L, Druker BJ, Marceau N: Down-regulation of cytokeratin 14 gene expression by the polyoma virus middle T antigen is dependent on c-src association but independent of full transformation in rat liver nonparenchymal epithelial cells. Cell Growth Differ 1996, 7:737–743
33. Bosser BG, Gores GJ: Liver cell necrosis: cellular mechanisms and clinical implications. Gastroenterology 1995, 108:252–275
34. Kawahara H, French SW: Role of cytoskeleton in canalicular contraction in cultured differentiated hepatocytes. Am J Pathol 1990, 136: 521–532
35. Tsukada N, Ackerley CA, Phillips MJ: The structure and organization of the bile canalicular cytoskeleton with special reference to actin and actin-binding proteins. Hepatology 1995, 21:1106–1113
36. Fausto N, Webber EM: Mechanismes of growth regulation in liver regeneration and hepatic carcinogenesis. Prog Liver Dis 1993, 11: 115–137
37. Mitchell P: Keilin's respiratory chain concept and its chemosmotic consequences. Science 1979, 206:1148–1159
38. King H, Hawtof DB: Accidental intra-arterial injection of ether. JAMA 1963, 184:241–242
39. Loranger A, Tuchweber B, Gicquaud C, St-Pierre S, Côté MG: Toxicity of peptides of Amanita virosa mushrooms in mice. Fundam Appl Toxicol 1985, 5:114–1152
40. Arias IM, Che M, Gatmaitan Z, Leveille C, Nishida T, St. Pierre M: The Biology of the Bile Canaliculus. Hepatology 1993, 17:318–329
41. Brown SES, Quattrochi LC, Guzelian PS: Characterization of a pretranscriptional pathway for induction by phenobarbital of cytochrome

P450 3A23 in primary cultures of adult rat hepatocytes. Arch Biochem Biophys 1997, 342:137–142

42. Ku NO, Weight TL, Terrault NA, Gish R, Omary MB: Mutation of human keratin 18 in association with cryptogenic cirrhosis. J Clin Invest 1997, 99:19–23
43. Greeve ML, Ferrell MK, Combs C, Roberts J, Ascher N, Wright TL: Cirrhosis of undefined pathogenesis: absence of evidence for unknown viruses or autoimmune processes. Hepatology 1993, 17:593–598
44. Omary MB, Ku NO: Intermediate filament proteins of the liver: emerging disease association and functions. Hepatology 1997, 25:1043–1048